



Molecular binding thermodynamics of spherical guests by β -cyclodextrins bearing aromatic substituents



Nan Li, Yong Chen, Ying-Ming Zhang, Li-Hua Wang, Wen-Zhao Mao, Yu Liu*

Department of Chemistry, State Key Laboratory of Elemento-Organic Chemistry, Nankai University, Collaborative Innovation Center of Chemical Science and Engineering, Tianjin 300071, PR China

ARTICLE INFO

Article history:

Received 30 September 2013

Received in revised form

21 November 2013

Accepted 22 November 2013

Available online 1 December 2013

Keywords:

β -Cyclodextrin

Thermodynamic

Self-inclusion

Borneol

Camphor

ABSTRACT

The molecular binding behaviors of two β -cyclodextrin (β -CD) derivatives bearing 1,2,3-triazole moieties, i.e. mono-6-deoxy-6-{4-(8-oxymethylquinolino)[1,2,3]triazolyl}- β -CD (**1**) and mono-6-deoxy-6-{4-(8-oxymethylnaphthol)[1,2,3]triazolyl}- β -CD (**3**), and their analogs without 1,2,3-triazole moieties, i.e. mono-6-deoxy-6-(8-oxymethylquinolino)- β -CD (**2**) and mono-6-deoxy-6-(8-oxymethylnaphthol)- β -CD (**4**) toward spherical guests (\pm)-borneol and (\pm)-camphor were investigated to elucidate how substituent moiety of host affects the binding abilities by 2D NMR as well as microcalorimetric titrations in aqueous phosphate buffer solution (pH 7.20) at 298.15 K. The binding modes of host–guest interactions obtained from 2D NMR displayed that host CDs without triazole moieties gave better induce-fit efficiency between hosts and guests, leading to stronger binding abilities. Thermodynamically, the inclusion complexation was driven by enthalpy with the stoichiometry of 1:1. Another factor contributed to the enhanced binding abilities was the enthalpy gain with the smaller entropy loss.

© 2013 Elsevier B.V. All rights reserved.

1. Introduction

Cyclodextrins (CDs) are cyclic oligosaccharides, formed from α -1,4 glucosidic bonds of a number of glucose units. Due to their hydrophilic outer surface and hydrophobic inner cavity, they offer the advantage of encapsulating various organic guests within their hydrophobic cavities to form host–guests complexes through the contribution of many intermolecular weak interactions, such as van der Waals, hydrophobic, hydrogen-bonding, dipole–dipole, and electrostatic interactions [1–4]. Moreover, introduction of diverse substituents may alter both the physicochemical properties of the CDs and the binding ability between CDs and guest molecules [5–7]. Therefore, great efforts have been put into designing and developing of novel CD derivatives. In addition, “click chemistry” [8] was widely studied in various fields, particularly in designing new molecules and macromolecules under very mild reaction conditions and high yield [9,10]. In the present work, we synthesized a series of quinoline- and naphthol-modified β -CD derivatives with and without triazole moieties (Fig. 2), and investigated their binding behaviors toward (\pm)-borneol and (\pm)-camphor (Fig. 1), which are bicyclic terpenoids possessing the advantages of biological functions such as antibacterial, antispasmodic, choleric, and tranquilizing effects [11]. It was our special interest to examine

the effects of different conformation on binding abilities of β -CD derivatives from the viewpoints of binding geometry and binding thermodynamics.

2. Experimental

2.1. Materials

All chemicals were used as reagent grade unless noted. β -CD was recrystallized twice from water and dried in vacuo at for 24 h. Camphor and borneol enantiomers were commercially available and used as received. Phosphate buffer solution of pH 7.20 ($I=0.1$ M, 3% DMSO) was used for ITC experiments. Mono[6-*O*-(*p*-toluenesulfonyl)]- β -CD (6-OTs- β -CD) **7** was prepared by the reaction of native β -CD with *p*-toluenesulfonyl chloride in NaOH aqueous solution in ca. 10% yield [12]. 6-Deoxy-6-azido- β -CD **8** was prepared according to the literature procedure [13]. Crude DMF was stirring in CaH_2 for three days and then distilled under reduced pressure prior to use.

2.2. Synthesis of 8-propargyloxynaphthalene (**6**)

A mixture of 1-naphthol **5** (2.4 g, 0.015 mol), K_2CO_3 (6.2 g, 0.045 mol) and propargyl bromide (80%, w/w solution in toluene, 3.6 mL, 0.045 mol) in 40 mL of acetone was refluxed overnight. Insoluble precipitates were removed by filtration, and the filtrate was evaporated in vacuo. The residue was dissolved in CH_2Cl_2

* Corresponding author.

E-mail address: yuliu@nankai.edu.cn (Y. Liu).

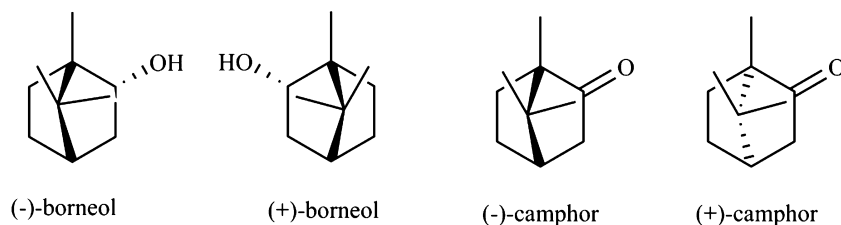


Fig. 1. Structures of guest molecules.

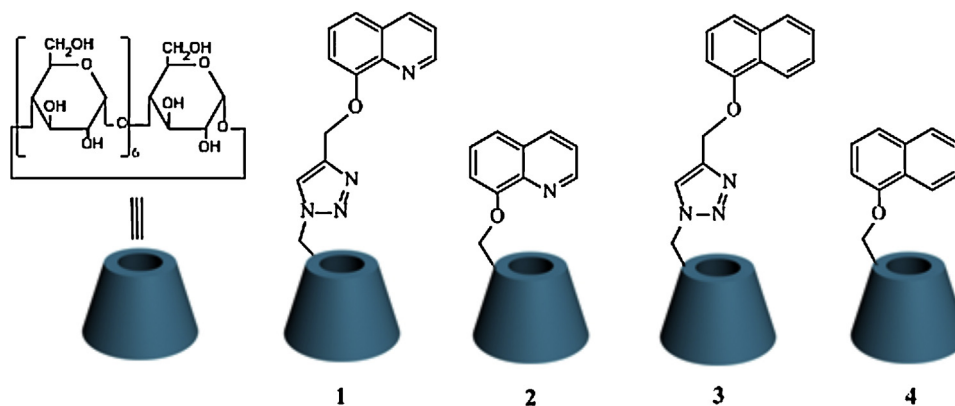


Fig. 2. Structures of host molecules.

(100 mL), and the organic layer was extracted with 1 M HCl solution (2×50 mL) and brine. The yellow solution was dried under reduced pressure and further purified by flash column chromatography using PE/ CH_2Cl_2 (10:1, v:v) as eluent to give the product as a colorless oil with a yield of 79% ($R_f = 0.4$). $^1\text{H NMR}$ (400 MHz, CDCl_3 , TMS, ppm): $\delta = 2.55$ (t, $J = 2.4$ Hz, 1H; H of $\text{CH}=\text{C}-$), 4.91 (d, $J = 2.4$ Hz, 2H; H of $\text{CH}=\text{C}-\text{CH}_2-$), 6.95 (d, $J = 7.6$, 1H; H of naphthalene), 7.39 (t, $J = 8.0$ Hz, 1H; H of naphthalene), 7.45–7.53 (m, 3H; H of naphthalene), 7.81 (dd, $J = 6.2$, 3.2 Hz, 1H; H of naphthalene), 8.32–8.24 (m, 1H; H of naphthalene). Anal. Calcd. for $\text{C}_{13}\text{H}_{10}\text{O}$: C, 85.69%; H, 5.53%. Found: C, 85.40%; H, 5.73%. EI-MS: 182 $[\text{M}+\text{H}]^+$.

2.3. Synthesis of mono-6-deoxy-6-{4-(8-oxymethylnaphthol)}[1,2,3]triazolyl}- β -CD (**3**)

8-Propargyloxynaphthalene **6** (328 mg, 1.80 mmol) in 15 mL of THF was added to a solution of $\text{CuSO}_4 \cdot 5\text{H}_2\text{O}$ (600 mg, 2.40 mmol) and mono-6-deoxyl-6-azido- β -CD **8** (1.39 g, 1.20 mmol) in 35 mL of water. The mixture was kept at 50°C for 10 min, and then sodium ascorbate (1.42 g, 7.20 mmol) was added. The color of the mixture turned orange immediately. Then, the mixture was heated at 50°C under an atmosphere of N_2 overnight. After cooled to room temperature, insoluble precipitates were removed by filtration, and the filtrate was evaporated in vacuo. The residue was dissolved in a small amount of water, and washed with 300 mL of acetone for at least three times. After separation by column chromatography (silica gel) using $n\text{-PrOH}:\text{H}_2\text{O}:\text{NH}_3 \cdot \text{H}_2\text{O}$ (6:3:1, v:v:v) as eluent, **3** was obtained as a white solid with a yield of 70% ($R_f = 0.4$). $^1\text{H NMR}$ (400 MHz, $\text{DMSO}-d_6$, ppm) $\delta = 3.65$ (dd, $J = 40.2$, 19.4 Hz, 24H; C-6 H of β -CD), 4.54 (dd, $J = 41.9$, 20.9 Hz, 6H; O-6 H of β -CD), 4.96–4.78 (m, 7H; C-1 H of β -CD), 5.30 (s, 2H; H of $-\text{CH}_2-$), 5.97–5.62 (m, 14H; O-2, 3 H of β -CD), 7.19 (d, $J = 7.7$ Hz, 1H; H of naphthalene), 7.55–7.41 (m, 4H; H of naphthalene), 7.87 (d, $J = 8.2$ Hz, 1H; H of naphthalene), 8.11 (d, $J = 8.0$ Hz, 1H; H of naphthalene), 8.28 (s, 1H; H of triazole). Anal. Calcd. for $\text{C}_{55}\text{H}_{79}\text{N}_3\text{O}_{35} \cdot 2\text{H}_2\text{O}$: C, 47.93%; H, 6.07%; N, 3.05%. Found: C, 47.90%; H, 6.27%; N, 3.12%. ESI-MS: 1364 $[\text{M}+\text{H}]^+$.

2.4. Synthesis of mono-6-deoxy-6-(8-oxymethylnaphthol)- β -CD (**4**)

Anhydrous K_2CO_3 (0.47 g, 3.0 mmol) was added to a solution of 8-hydronaphthalene (516 mg, 3.0 mmol) in dry DMF (12 mL). The mixture was stirred for 2 h at room temperature under nitrogen. Then, 6-OTs- β -CD **7** (1.9 g, 1.5 mmol) in dry DMF (20 mL) was

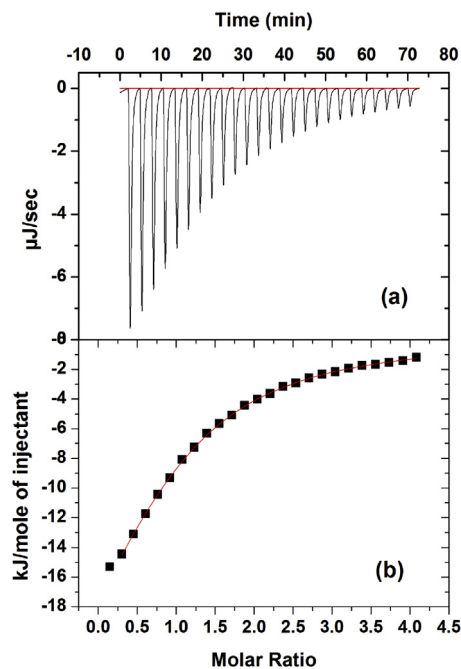


Fig. 3. Microcalorimetric titration of host **1** with (-)-borneol in phosphate buffer solution (pH=7.20, $I = 0.1$ M, 3% DMSO) at 298.15 K. (a) Raw data for sequential 25 injections (10 μL /injection) of (-)-borneol solution (2.00 mM) into host **1** solution (0.094 mM). (b) Apparent reaction heat obtained from the integration of the calorimetric traces.

added dropwise with stirring, and the mixture was heated to 80 °C for 24 h. The resultant solution was evaporated under a reduced pressure to give yellow powder, which was dissolved in a minimum amount of hot water, and then the solution was poured into acetone (200 mL). After separation by column chromatography (silica gel) using n-PrOH:H₂O:NH₃·H₂O (6:3:1, v:v:v) as eluent, **4** was obtained as a white solid with a yield of 20% ($R_f=0.4$). ¹H NMR (400 MHz, DMSO-*d*₆, ppm) δ =3.64 (dd, $J=54.7, 25.1$ Hz, 27H; C2-6 H of β -CD), 4.45 (dd, $J=39.5, 22.5$ Hz, 6H; O-6 H of β -CD), 4.86 (t, $J=30.2$ Hz, 7H; C-1 H of β -CD), 5.75 (d, $J=30.0$ Hz, 14H; O-2, 3H of β -CD), 6.96 (d, $J=7.4$ Hz, 1H; H of naphthalene), 7.36–7.57 (m, 4H, 1H; H of naphthalene), 7.86 (d, $J=6.5$ Hz, 1H; H of naphthalene), 8.19 (d, $J=6.9$ Hz, 1H; H of naphthalene). Anal. Calcd. for C₅₂H₇₆O₃₅·4H₂O: C, 46.85%; H, 6.35%. Found: C, 47.10%; H, 6.26%. ESI-MS: 1283 [M+Na]⁺.

2.5. Microcalorimetric titration

Microcal VP-ITC titration microcalorimeter allows us to simultaneously determine the binding constant and the enthalpic change from a single titration curve. The VP-ITC instrument was calibrated chemically by the measurement of the complexation reaction of β -CD with cyclohexanol, and the obtained thermodynamic data were in good agreement (error <2%) with the literature data. All

ITC experiments were performed in aqueous phosphate buffer solution (pH 7.20, $I=0.1$ M) at atmospheric pressure and 298.15 K, and 3% DMSO was added into the phosphate buffer to increase the solubility of hosts **3** and **4**. All solutions were degassed by a Thermo Vac accessory before titration experiments. Each microcalorimetric titration experiment consisted 25 successive injections of a constant volume (10 μ L/injection) of guest solution into the reaction cell (1.4227 mL) charged with host solution in the same buffer. Typical titration curves were shown in Fig. 3. Each titration of guest molecules into the sample cell gave a reaction heat caused by the formation of inclusion complex between CDs and guest molecules. The reaction heat decreased after each injection of guest molecules because less and less CDs were available to form inclusion complexes. The dilution heat of host solution when added to the pure buffer solution in the absence of CDs was determined in each run. The dilution heat determined in these control experiments were subtracted from the apparent reaction heat measured in titration experiments to give the net reaction heat.

The net heat in each run was analyzed by using “one set of binding sites” model with ORIGIN software which provided by Microcal Inc. to determine the binding stoichiometry (N), binding constant (K_S), and reaction enthalpic changes (ΔH°) from the titration curve. Knowledge of the binding constant (K_S) and the reaction enthalpic changes (ΔH°) enabled the calculation of standard Gibbs

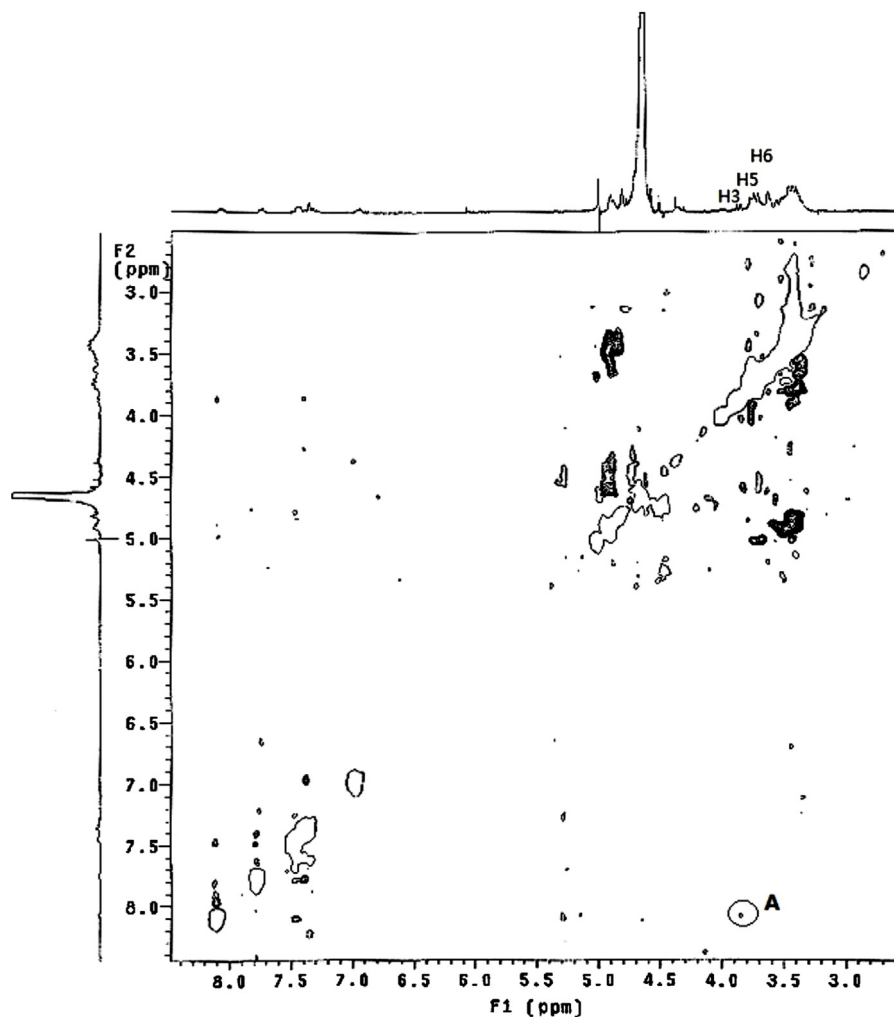


Fig. 4. ROESY spectrum of host **4** in D₂O with a mixing time of 280 ms at 298.15 K. (For interpretation of the references to color in this figure legend, the reader is referred to the web version of this article.)

Table 1

Complex stability constants (K_S/M^{-1}), enthalpic changes (ΔH°), entropic changes ($T\Delta S^\circ$) and Gibbs free energy changes (ΔG°) for 1:1 intermolecular complexation of (\pm)-borneol and (\pm)-camphor with host CDs in phosphate buffer solution (pH 7.20, $I=0.1$ M, 3% DMSO) at 298.15 K.

Guests	Hosts	$K_S (M^{-1})$	$\Delta G^\circ (kJ mol^{-1})$	$\Delta H^\circ (kJ mol^{-1})$	$T\Delta S^\circ (kJ mol^{-1})$
(-)-Borneol	β -CD	$(96.36 \pm 3.54) \times 10^2$	-22.73 ± 0.18	-20.81 ± 0.98	1.93
	1	$(15.86 \pm 0.28) \times 10^3$	-23.97 ± 0.04	-25.80 ± 0.18	-1.82
	2	$(22.31 \pm 0.62) \times 10^3$	-24.82 ± 0.07	-29.64 ± 0.17	-4.81
	3	$(10.08 \pm 0.35) \times 10^3$	-22.85 ± 0.09	-23.09 ± 0.04	-0.24
	4	$(34.89 \pm 0.84) \times 10^3$	-25.93 ± 0.06	-27.97 ± 0.21	-2.03
(+)Borneol	β -CD	$(62.69 \pm 3.07) \times 10^2$	-21.67 ± 0.12	-32.70 ± 0.68	-10.97
	1	$(15.74 \pm 0.18) \times 10^3$	-23.95 ± 0.03	-25.04 ± 0.11	-1.08
	2	$(19.04 \pm 0.00) \times 10^3$	-24.43 ± 0.00	-31.91 ± 0.45	-7.48
	3	$(10.23 \pm 0.01) \times 10^3$	-22.89 ± 0.03	-21.11 ± 0.11	1.55
	4	$(40.34 \pm 2.28) \times 10^3$	-26.28 ± 0.14	-25.20 ± 1.40	1.08
(-)-Camphor	β -CD	$(23.64 \pm 2.37) \times 10^2$	-19.24 ± 0.25	-26.70 ± 1.29	-7.45
	1	$(47.76 \pm 0.78) \times 10^2$	-21.00 ± 0.04	-18.02 ± 0.88	2.97
	2	$(52.59 \pm 1.16) \times 10^2$	-21.24 ± 0.05	-20.69 ± 0.33	0.55
	3	$(26.18 \pm 0.70) \times 10^2$	-19.51 ± 0.07	-15.49 ± 0.41	4.02
	4	$(83.24 \pm 5.70) \times 10^2$	-22.37 ± 0.17	-19.27 ± 0.27	3.10
(+)Camphor	β -CD	$(23.77 \pm 0.66) \times 10^2$	-19.27 ± 0.07	-22.58 ± 1.24	-3.30
	1	$(35.54 \pm 0.96) \times 10^2$	-20.27 ± 0.07	-19.28 ± 0.01	0.99
	2	$(42.70 \pm 3.58) \times 10^2$	-20.71 ± 0.21	-25.89 ± 1.29	-5.15
	3	$(31.26 \pm 0.59) \times 10^2$	-19.95 ± 0.05	-16.77 ± 0.02	3.19
	4	$(57.19 \pm 1.62) \times 10^2$	-21.44 ± 0.07	-22.07 ± 0.34	-0.63

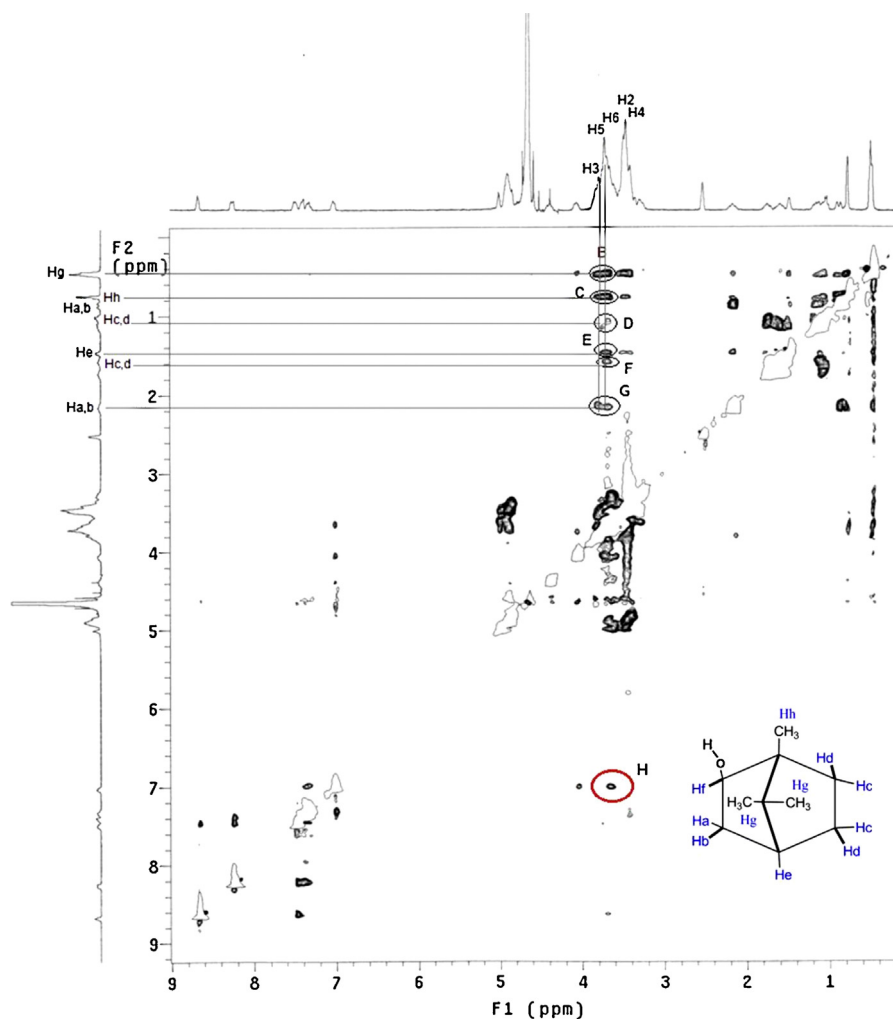


Fig. 5. ROESY spectrum of **2**/(-)-borneol ($[2]=[(\text{-})\text{-borneol}]=1.0$ mM) in D_2O (3% DMSO) with a mixing time of 280 ms at 298.15 K. (For interpretation of the references to color in this figure legend, the reader is referred to the web version of this article.)

free energy changes (ΔG°) and entropic change (ΔS°), according to equation

$$\Delta G^\circ = -RT \ln K_S = \Delta H^\circ - T\Delta S^\circ$$

where R is the gas constant and T is the absolute temperature.

To check the accuracy of calculated thermodynamic quantities, we carried out several independent titration runs to afford self-consistent thermodynamic parameters, and their average values were listed in Table 1.

3. Results and discussion

3.1. Circular dichroism spectra and fluorescence emission spectra

Generally, the proximity of an achiral chromophore to CD cavity gives rise to the induced circular dichroism (ICD) signals at wavelengths absorbed by the chromophore, and the sign of ICD signals mainly depends on the orientation of transition dipole moment of chromophore with respect to the axis of CD [14]. As seen from Supplementary Figure S8, the circular dichroism spectra of hosts **1** and **2** displayed the weak ($|\Delta\epsilon| < 0.5 \text{ M}^{-1} \text{ cm}^{-1}$), but opposite, ICD signals; that is, host **1** gave positive ICD signals but host **2** negative signals. This result can be rationalized by our previous report where the side arm of host **2** was self-included in, but that of host **1** located outside the β -CD cavity [15]. In addition, hosts **3** and **4** gave weak,

but positive ICD signals, like that of host **1**. These weak positive ICD signals indicated that the side arms of hosts **3** and **4** may also be located distant from the narrow opening of β -CD cavity. In fluorescence experiments, the fluorescence intensity of hosts **1**, **3**, or **4** slightly changed, but the shape of emission peak almost unchanged, after the addition of guest molecules, indicating the conformation of hosts **1**, **3**, or **4** was maintained upon guest complexation. However, both the shape and intensity of the emission peak of host **2** showed the obvious changes with the addition of guest molecules, indicating that host **2** may undergo a conformational change upon guest complexation.

3.2. 2D NMR

2D NMR spectroscopy is an essential method for the investigation of interactions between CDs and guest molecules, because two protons which are closely located in space can produce an NOE cross-peak between the relevant protons in NOESY or ROESY spectra. Moreover, 2D ROESY experiment is suitable for the detailed spatial interaction and the corresponding three-dimensional geometry information in host-guest complex study [16]. Fig. 4 gave the ROESY spectrum of host **4** in D_2O , which displayed the NOE correlations between H5/H6 protons of β -CD and protons of the naphthalene moiety of host **4** (cross-peaks A). In addition, no NOE correlation between H3 protons of β -CD

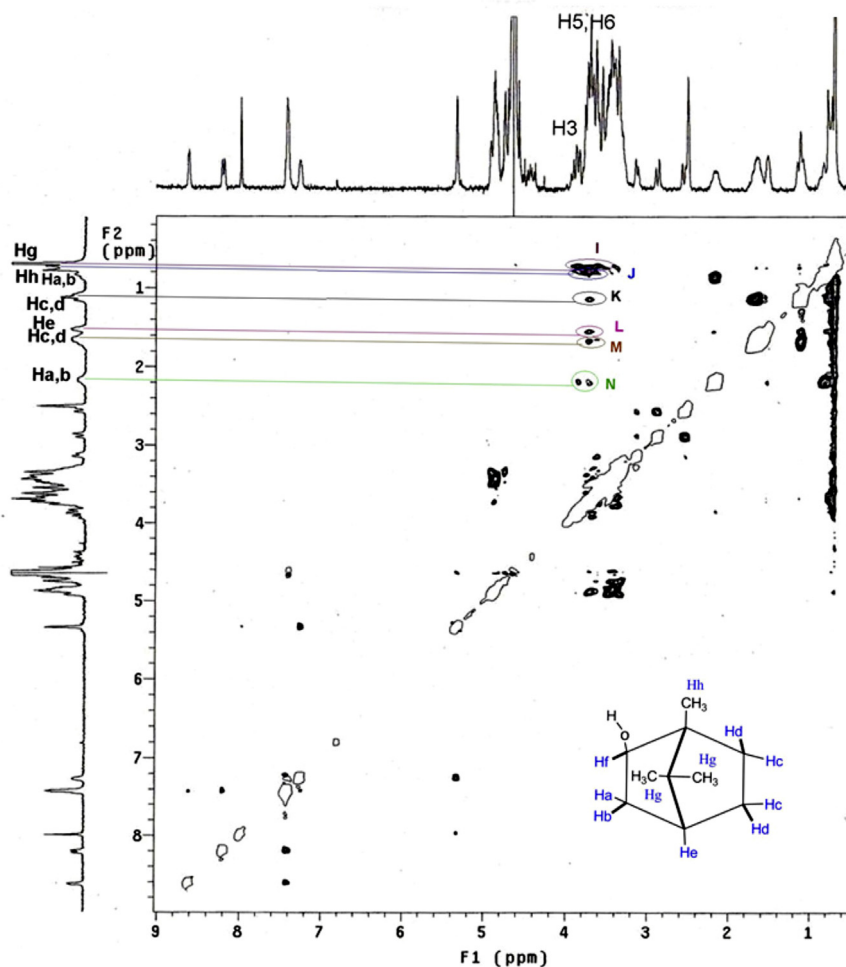


Fig. 6. ROESY spectrum of **1**/(-)-borneol ($[\text{1}] = [(-)\text{-borneol}] = 1.0 \text{ mM}$) in D_2O (3% DMSO) with a mixing time of 280 ms at 298.15 K. (For interpretation of the references to color in this figure legend, the reader is referred to the web version of this article.)

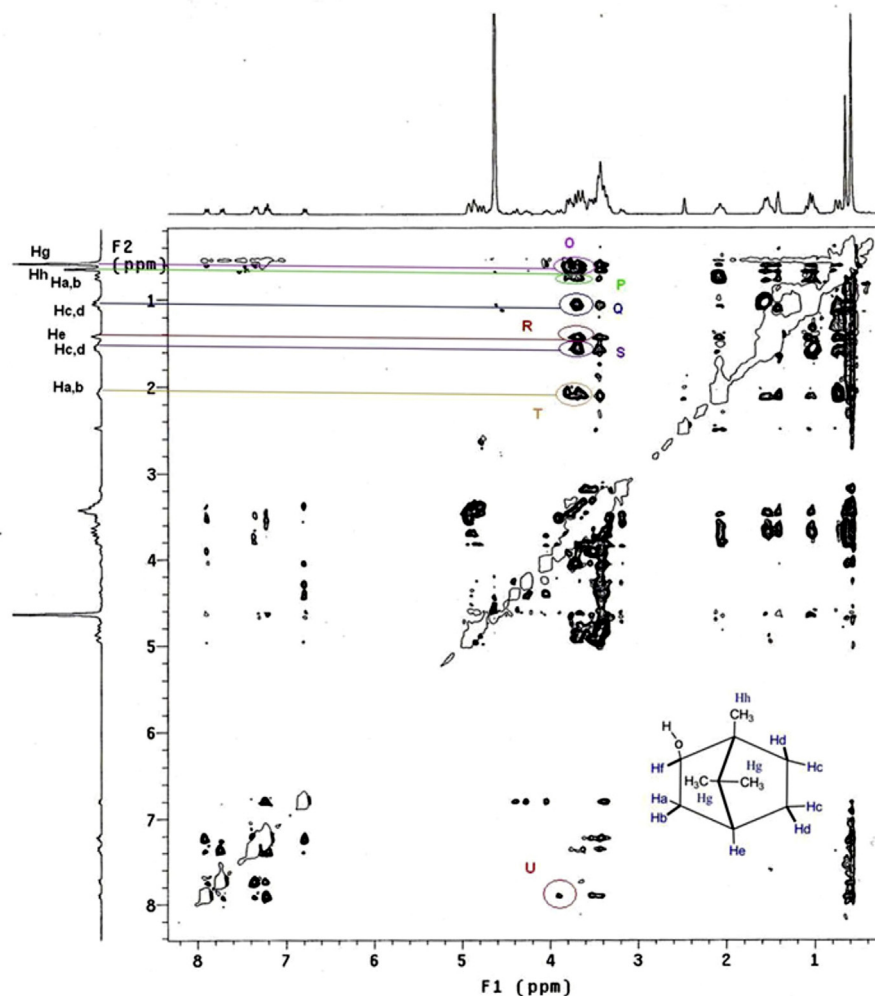


Fig. 7. ROESY spectrum of **4**/(-)-borneol ($[4] = [(-)\text{-borneol}] = 1.0 \text{ mM}$) in D_2O (3% DMSO) with a mixing time of 250 ms at 298.15 K. (For interpretation of the references to color in this figure legend, the reader is referred to the web version of this article.)

and naphthalene protons could be observed. It is well-known that H5/H6 protons are located near the narrow side of the CD cavity, whereas H3 protons are near the wide side. This information indicated that the naphthalene moiety of **4** shallowly penetrated into the cavity of β -CD from the narrow side. In contrast, no NOE correlation between naphthalene protons of **3** and interior protons (H3/H5/H6) of β -CD cavity could be observed, indicating the naphthalene substituent of **3** was located outside the β -CD cavity. In our previous report, host **2** adopted a self-included conformation but host **1** adopted a self-excluded one [15]. Therefore, we deduced that host CDs without triazole group would form self-included monomer, but the introduction of triazole group would prevent the self-penetration of substituent moieties into CD cavities.

Fig. 5 shows the ROESY spectrum of an equimolar mixture of host **2** with (-)-borneol. The cross-peak H was assigned to NOE correlation between H3/H5 protons of β -CD and protons of the quinoline moiety. This indicated that the quinoline moiety was still located in the β -CD cavity after the guest inclusion. Meanwhile, we also found that the strength of NOE correlations of quinoline protons of **2** with H5/H6 protons of β -CD became stronger than that with H3 protons. Hence, we indicated that the quinoline moiety of **2** partly moved to the narrow opening of β -CD. In addition, cross-peaks between protons of (-)-borneol and interior protons of β -CD cavity were marked as peaks B, C, D, E, F, and G. Among them, the peak B was assigned to NOE correlations between H_g protons of (-)-borneol and H3/H5 protons of β -CD. The peak C was

assigned to NOE correlations between H_h protons of (-)-borneol with H3/H5/H6 protons of β -CD. Peaks D and F were assigned to NOE correlations between H_c/H_d protons of (-)-borneol and H3/H5/H6 protons of β -CD, where H5/H6 protons gave stronger NOE correlations than H3 protons. The peak E was assigned to NOE correlations between H_e protons of (-)-borneol and H5/H6 protons of β -CD. The peak G was assigned to NOE correlations between H_a/H_b protons of (-)-borneol and H3/H5/H6 protons of β -CD, where H3 protons gave stronger NOE correlations than H5/H6 protons. According to these NOE signals, we deduced that host **2** adopted a co-inclusion mode upon complexation with (-)-borneol, where the guest molecule entered the β -CD cavity from the wide side and the quinoline moiety was self-included in the β -CD cavity from the narrow side.

The ROESY spectrum of an equimolar mixture of host **1** with (-)-borneol was shown in Fig. 6. We could also see NOE correlation between protons of (-)-borneol and interior protons of β -CD cavity. The cross-peak I was assigned to NOE correlations between H_g protons of (-)-borneol and H3/H5/H6 protons of β -CD, and the cross-peak J was assigned to NOE correlations between H_h protons of (-)-borneol and H3/H5 protons of β -CD. Moreover, peaks K and M were assigned to NOE correlations between H_c/H_d protons of (-)-borneol and H5/H6 protons of β -CD, and the peak L was assigned to NOE correlations between H_e protons of (-)-borneol and H5/H6 protons of β -CD. The peak N was assigned to NOE correlations between H_a/H_b protons of (-)-borneol and H3/H5 protons of β -CD, where

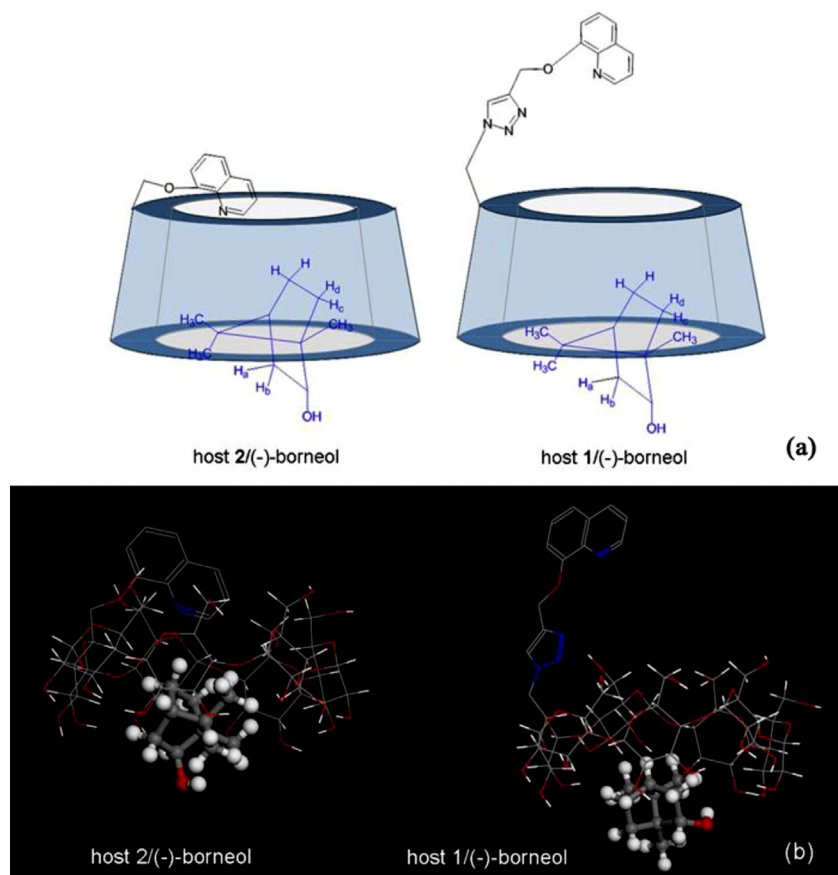


Fig. 8. (a) Possible binding modes of hosts **2** and **1** with (–)-borneol. (b) Structures of **2**/(–)-borneol and **1**/(–)-borneol based on molecular modeling study. The structures were colored by atom type: gray, carbon atoms; white, hydrogen atoms; red, oxygen atoms; blue, nitrogen atoms. (For interpretation of the references to color in this figure legend, the reader is referred to the web version of this article.)

H3 protons gave stronger NOE correlations than H5 protons. As mentioned previously, host **1** was not self-included. Therefore, we deduced that the (–)-borneol guest entered the β -CD cavity through the wide side, and the substituent moiety of host **1** was still located out of the β -CD cavity. The similar binding mode was also observed in the inclusion complexation of host **3**. The possible molecular binding modes of hosts **2** and **1** with (–)-borneol were depicted in Fig. 8(a).

Fig. 7 gave the ROESY spectrum for the complex between host **4** and (–)-borneol. The cross-peak O corresponded to NOE correlations between H_g protons of (–)-borneol and H3/H5/H6 protons of β -CD, and the cross-peak P was assigned to NOE correlations between H_h protons of (–)-borneol and H3/H5/H6 protons of β -CD. Meanwhile, peaks Q and S were assigned to NOE correlations between H_c/H_d protons of (–)-borneol and H5/H6 protons of β -CD, and the peak R was assigned to NOE correlations between H_e protons of (–)-borneol and H5/H6 protons of β -CD. In addition, the peak T was assigned to NOE correlations between H_a/H_b protons of (–)-borneol and H3/H5/H6 protons of β -CD, where H3 protons gave stronger NOE correlations than H5/H6 protons. Moreover, we could still find the NOE correlations (peak U) between protons of β -CD and protons of the naphthalene moiety of host **4**, thus we could deduce that naphthalene moiety of **4** still partially included into the cavity of β -CD from the narrow opening and the guest molecule entered the cavity of host **4** from the wide opening.

3.3. Binding stoichiometry

In ITC experiments, all of host–guest binding gave a 1:1 stoichiometry with “N” values in the curve fitting results varying from 0.9

to 1.1 [17–21]. Moreover, the CPK (Corey–Pauling–Koltun) molecular modeling study showed that each β -CD cavity could only accommodate one borneol or camphor molecule (Fig. 8b). Therefore, a fixed 1:1 binding stoichiometry was used in the curve-fitting analysis of calorimetric titration.

3.4. Binding ability

As reported, substituents of host CDs were not protonated at a neutral environment [15,22]. Therefore, non-covalent weak interactions such as hydrophobic interaction, van der Waals interaction, and hydrogen bonding should be main driving forces of the host–guest inclusion complexation, and the strength of these weak interactions are greatly governed by the size/shape fitting efficiency between host and guest [11]. As shown in Table 1, binding abilities of hosts **1–4** toward borneol were higher than toward camphor. Possessing a hydroxyl group at the C-2 position, borneol could give stronger hydrogen bond interactions with numerous hydroxyl groups of CD cavities. While, hydrogen bond interactions should be weaker between camphor, which possesses a carbonyl group at the C-2 position, and host CDs. This result was also verified by thermodynamic data, where most of host/borneol bindings showed more negative enthalpic changes than host/camphor ones.

Compared with native β -CD, hosts **1–4** exhibited larger K_S values toward borneol and camphor. K_S values for bindings of hosts **1–4** were 1.1–6.4 times higher toward borneol and 1.3–3.5 times higher toward camphor than corresponding values of β -CD. To visualize and easily discuss the binding ability, the order of

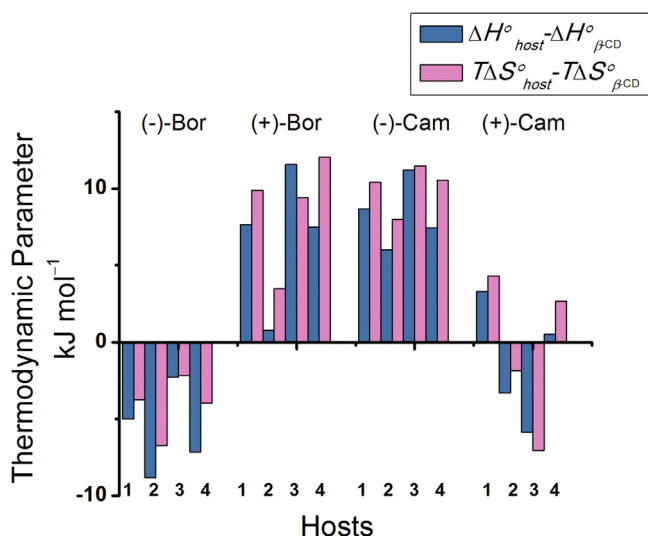


Fig. 9. Enthalpic ($\Delta H^{\circ}_{\text{host}} - \Delta H^{\circ}_{\beta\text{-CD}}$) and entropic changes ($T\Delta S^{\circ}_{\text{host}} - T\Delta S^{\circ}_{\beta\text{-CD}}$) for inclusion complexations of (\pm)-borneol and (\pm)-camphor with hosts **1–4** in phosphate aqueous buffer solutions (pH = 7.20, $I = 0.1$ M, 3% DMSO) at 298.15 K.

complex stability constants for (\pm)-borneol and (\pm)-camphor by native β -CD and hosts **1–4** were shown as follows:

- (–)-Borneol: **4** > **2** > **1** > **3** > β -CD;
 (+)-Borneol: **4** > **2** > **1** > **3** > β -CD;
 (–)-Camphor: **4** > **2** > **1** > **3** > β -CD;
 (+)-Camphor: **4** > **2** > **1** > **3** > β -CD.

It was interesting to note that, host **2** (or **4**) gave obviously stronger binding abilities toward guest molecules than host **1** (or **3**). In the previous section, 2D NMR studies demonstrated that host **2** (or **4**) adopted a co-inclusion binding mode upon complexation with guest molecules. This binding mode not only decreased the effective volume of β -CD cavity to some extent and thus led to the higher size-fit efficiency between host and guest [23], but also enabled additional non-covalent interactions between the substituent group and the accommodated guest molecules. On the other hand, the existence of triazole moiety in host **1** (or **3**) increased the distance from the substituent group to the accommodated guest molecule. Due to the joint contribution of these factors, host CDs without triazole moieties showed higher binding abilities than host CDs with triazole moieties.

3.5. Binding thermodynamic parameters

From data presented in Table 1, large negative enthalpic changes ($\Delta H^{\circ} < 0$) were observed in all bindings of hosts **1–4** with borneol and camphor, accompanied by either positive or negative entropic changes. This result indicated that bindings of host CDs with guest molecules were driven by enthalpy, and van der Waals interactions and hydrogen bonds were mainly responsible for inclusion complexations. From data of enthalpic changes (ΔH°) and entropic changes ($T\Delta S^{\circ}$) between hosts and guests in Table 1, we could see that bindings of borneol with host CDs displayed more negative enthalpic changes (-20.81 kJ mol $^{-1}$ to -32.70 kJ mol $^{-1}$) than those of camphor (-15.49 kJ mol $^{-1}$ to -26.70 kJ mol $^{-1}$). This is consistent with our previous deduction that borneol could give stronger hydrogen bonds with host CDs.

In addition, from a comparison of differential reaction enthalpic and entropic changes, in Fig. 9 we found that nearly all of differential reaction enthalpic changes ($\Delta H^{\circ}_{\text{Hosts 1–4}} - \Delta H^{\circ}_{\beta\text{-CD}}$)

were more negative than differential entropic changes ($T\Delta S^{\circ}_{\text{Hosts 1–4}} - T\Delta S^{\circ}_{\beta\text{-CD}}$). Therefore, it may infer that enhanced binding abilities of hosts **1–4** toward with borneol and camphor were mainly attributed to favorable enthalpic contributions but not entropic contributions. In another word, it were van der Waals interactions and hydrogen bonds, but not hydrophobic interactions or desolvation effects, that led to stronger binding abilities of hosts **1–4** than native β -CD.

4. Conclusion

In the present investigation, studies of binding behaviors of two β -CD derivatives bearing triazole groups and their analogs without triazole groups demonstrated that host CDs showed higher binding abilities than native β -CD. Thermodynamically, the binding behaviors of four host CDs toward guest molecules were entirely driven by favorable enthalpic changes, accompanied by unfavorable entropic changes. In addition, the hydrogen-bonding interactions and van der Waals interactions were the main driven forces governing the host–guest binding. Moreover, the formation of self-included monomers could not only increase binding abilities but also strengthen desolvation effects of hosts and guests to some extent because the self-included conformation led to the better induced-fit effect in the host–guest co-inclusion binding mode.

Acknowledgments

We thank NNSFC (21272125 and 21102075), Program for New Century Excellent Talents in University (NCET-10-0500), and the Specialized Research Fund for the Doctoral Program of Higher Education (20110031120014) for financial support.

Appendix A. Supplementary data

Supplementary data associated with this article can be found, in the online version, at <http://dx.doi.org/10.1016/j.tca.2013.11.021>.

References

- [1] (a) Y. Liu, Y. Chen, *Acc. Chem. Res.* **39** (2006) 681; (b) Y. Chen, Y. Liu, *Chem. Soc. Rev.* **39** (2010) 495.
- [2] M.V. Rekharsky, Y. Inoue, *Chem. Rev.* **98** (1998) 1875.
- [3] K.N. Houk, A.G. Leach, S.P. Kim, X.-Y. Zhang, *Angew. Chem. Int. Ed.* **42** (2003) 4872.
- [4] W. Tao, Y. Liu, B.-B. Jiang, S.-R. Yu, W. Huang, Y.-F. Zhou, D.-Y. Yan, *J. Am. Chem. Soc.* **134** (2012) 762.
- [5] R. Holm, J.C. Madsen, W. Shi, K.L. Larsen, L.W. Ståde, P.J. Westh, *Incl. Phenom. Macrocycl. Chem.* **69** (2011) 201.
- [6] C. Schönbeck, P. Westh, J.C. Madsen, K.L. Larsen, L.W. Ståde, R. Holm, *Langmuir* **26** (2010) 17949.
- [7] A.R. Khan, P. Forgo, K.J. Stine, V.T. D'Souza, *Chem. Rev.* **98** (1998) 1977.
- [8] (a) H.C. Kolb, M.G. Finn, K.B. Sharpless, *Angew. Chem.* **113** (2001) 2056; (b) H.C. Kolb, M.G. Finn, K.B. Sharpless, *Angew. Chem. Int. Ed.* **40** (2001) 2004.
- [9] V.V. Rostovtsev, L.G. Green, V.V. Fokin, K.B. Sharpless, *Angew. Chem. Int. Ed.* **41** (2002) 2596.
- [10] P.-A. Faugeras, B. Boëns, P.-H. Elchinger, F. Brouillette, D. Montplaisir, R. Zerrouki, R. Lucas, *Eur. J. Org. Chem.* (2012) 4087.
- [11] (a) N. Tabanca, N. Kirimer, B. Demirci, F. Demirci, K.H.C. Baser, *J. Agric. Food Chem.* **49** (2001) 4300; (b) F.J. Hammerschmidt, A.M. Clark, F.M. Soliman, E.A. El-Kashoury, M.M. Abd El-Kawy, A.M. El-Fishawy, *Planta Med.* **59** (1993) 68; (c) G. Buchbauer, W. Jäger, L. Jirovetz, F. Meyer, F. Dietrich, *Pharmazie* **47** (1992) 620.
- [12] R.C. Petter, J.S. Salek, C.T. Sikorski, G. Kumaravel, F.T. Lin, *J. Am. Chem. Soc.* **112** (1990) 3860.
- [13] C. Hocquet, J. Blu, C.K. Jankowski, S. Arseneau, D. Buisson, L. Mauclair, *Tetrahedron* **62** (2006) 11963.
- [14] (a) K. Harata, H. Uedaira, *Bull. Chem. Soc. Jpn.* **48** (1975) 375; (b) M. Kodaka, *J. Am. Chem. Soc.* **115** (1993) 3702.
- [15] N. Li, Y. Chen, Y.-M. Zhang, Z.-Q. Li, Y. Liu, *Sci. China Ser. B: Chem.* **40** (2010) 1355.

- [16] M.M. Al Omari, N.H. Daraghme, M.I. El-Barghouthi, M.B. Zughul, B.Z. Chowdhry, S.A. Leharne, A.A. Badwan, *J. Pharm. Biomed. Anal.* 50 (2009) 449.
- [17] Y. Liu, Y. Song, Y. Chen, Z.-X. Yang, F. Ding, *J. Phys. Chem. B* 109 (2005) 10717.
- [18] Y. Liu, L. Li, Y. Chen, L. Yu, Z. Fan, F. Ding, *J. Phys. Chem. B* 3 (2005) 584.
- [19] Y. Liu, R. Cao, Y. Chen, J.-Y. He, *J. Phys. Chem. B* 112 (2008) 1445.
- [20] Y. Liu, Y.-W. Yang, R. Cao, S.-H. Song, L.-H. Wang, *J. Phys. Chem. B* 112 (2008) 1445.
- [21] Y. Chen, F. Li, B.-W. Liu, B.-P. Jiang, H.-Y. Zhang, L.-H. Wang, Y. Liu, *J. Phys. Chem. B* 114 (2010) 16147.
- [22] Y.-M. Zhang, Y. Chen, Z.-Q. Li, N. Li, Y. Liu, *Bioorg. Med. Chem.* 18 (2010) 1415.
- [23] Y. Liu, Q. Zhang, Y. Chen, *J. Phys. Chem. B* 111 (2007) 12211.